Thermochemistry and Dissociative Photoionization of $Si(CH_3)_4$, $BrSi(CH_3)_3$, $ISi(CH_3)_3$, and $Si_2(CH_3)_6$ Studied by Threshold Photoelectron−Photoion Coincidence Spectroscopy†

Juan Z. Dávalos‡,§ and Tomas Baer‡

Department of Chemistry, University of North Carolina, Chapel Hill, North Carolina 27599-3290, and Instituto de Química-Física "Rocasolano", CSIC, Serrano 119, 28006, Madrid, Spain

Received: November 16, 2005; In Final Form: January 5, 2006

Threshold photoelectron−photoion coincidence spectroscopy (TPEPICO) has been used to study the dissociation kinetics and thermochemistry of Me_4Si, Me_6Si_2, and Me_3SiX, (X = Br, I) molecules. Accurate 0 K dissociative photoionization onsets for these species have been measured from the breakdown diagram and the ion time-of-flight distribution, both of them analyzed and simulated in terms of the statistical RRKM theory and DFT calculations. The average enthalpy of formation of trimethylsilyl ion, $\Delta_f H^\circ_{298K}(Me_3Si^+) = 617.3 \pm 2.3$ kJ/mol, has been determined from the measured onsets for methyl loss (10.243 ± 0.010 eV) from Me_4Si, and Br and I loss from Me_3SiBr (10.624 ± 0.010 eV) and Me_3SiI (9.773 ± 0.015 eV), respectively. The methyl loss onsets for the trimethyl halo silanes lead to $\Delta_f H^\circ_{298K}(Me_2SiBr^+) = 590.3 \pm 4.4$ kJ/mol and $\Delta_f H^\circ_{298K}(Me_5Si_2{}^+) = 487.6 \pm 6.2$ kJ/mol. The dissociative photoionization of $Me_3SiSiMe_3$ proceeds by a very slow Si−Si bond breaking step, whose rate constants were measured as a function of the ion internal energy. Extrapolation of this rate constant to the dissociation limit leads to the 0 K dissociation onset (9.670 ± 0.030 eV). This onset, along with the previously determined trimethylsilyl ion energy, leads to an enthalpy of formation of the trimethylsilyl radical, $\Delta_f H^\circ_{298}K(Me_3Si^\bullet) = 14.0 \pm 6.6$ kJ/mol. In combination with other experimental values, we propose a more accurate average value for $\Delta_f H^\circ_{298K}(Me_3Si^\bullet)$ of 14.8 ± 2.0 kJ/mol. Finally, the bond dissociation enthalpies (ΔH_{298K}) Si−H, Si−C, Si−X (X=Cl, Br, I) and Si−Si are derived and discussed in this study.

1. Introduction

The silicon chemistry continues to be an interesting field of study due not only to the technological applications (microelectronics) but also to the unique and surprising properties of silicon compounds. In particular, the organosilicon species are of key importance in processes such as chemical vapor deposition (CVD) of silicon films used in microelectronics as well as in protective coatings. A detailed understanding of CVD processes[1] requires kinetic and thermodynamic information such as bond energies. For instance, reactions including silylene (SiR_2) and silylidyne (SiR) species have been subject of many studies,[1−4] whereas, according to Krasnoperov et al.,[5] studies with the silyl radical (SiR_3) have been rather sparse.

The thermochemical properties of trimethylsilyl species (ion and radical) were investigated in the mid 1990s by Walsh and co-workers[6] and Marshall and co-workers.[7,8] Literature and new values were evaluated by taking into account the estimated errors in the enthalpy of formation measurements of Me_6Si_2 ($\Delta H^\circ_f = -303.7 \pm 5.5$ kJ/mol) and Me_4Si ($\Delta H^\circ_f = -233.2 \pm 3.2$ kJ/mol) obtained by Pilcher et al.[9] and Steele,[10] respectively. These values are quite different from those that were in the literature in the early 1980s.[11−13]

Auxiliary heats of formation are required to relate the measured reaction enthalpies to heats of formation. It is thus of great utility to obtain heats of formation and bond energies by several different routes so that the whole interconnecting network is tested. This is in fact the aim of the so-called active thermochemical tables,[14] which test the self-consistency of different measurements in a related series of compounds. Some years ago, a group of methylsilanes were investigated by threshold photoelectron photoion coincidence (TPEPICO) in which dissociation onsets for various dissociative photoionization reactions were measured.[15] In that study, the heats of formation of the following compounds were reported: $Me_3Si^\bullet$, Me_3Si^+, Me_2SiCl^+, Me_2SiBr^+ and Me_5Si^+. Because of the substantial advances in the TPEPICO technique[16−18] and the greatly increased reliability of the auxiliary heats of formation since that time (some differ by more than 30 kJ/mol), it seems appropriate to revisit this series of molecules to test the self-consistency of the energetic information on the alkyl and halogen substituted alkylsilanes. In addition, this study is a prelude for a similar investigation of the germanium analogues of these compounds.

The major experimental improvements of the current method over that in the 1984 study[15] is associated with the effect of energetic, or hot, electron contamination of the threshold electron signal. TPEPICO ion energy selection is based on energy conservation and the ion internal energy is given by $E_i = h\nu - IE - KE_{el}$, where $h\nu$ is the photon energy, IE is the molecule's ionization energy, and KE_{el} is the kinetic energy of the ejected electron. If the electron initial energy is zero, the ion gains the full energy of the photon. Thus, incomplete suppression of hot electrons results in a contamination of the ion signal by lower energy ions. The recent improvement in the TPEPICO method permits us to subtract the signal resulting from the hot electron coincidences thereby greatly improving the quality of the data. The major improvement in the data analysis is we now take

† Part of the "Chava Lifshitz Memorial Issue".
‡ University of North Carolina.
§ Instituto de Química-Física "Rocasolano".

10.1021/jp0566358 CCC: $33.50
Published on Web 02/17/2006

into account the thermal energy distribution of the sample gas whereas previously we simply corrected for this in an average manner. In addition, higher energy dissociation onsets can now be treated quantitatively and onset energies extracted with good precision.[17]

2. Experimental Section

A. TPEPICO Spectrometer. This study was performed on a threshold photoelectron photoion coincidence (TPEPICO) spectrometer[16−20] that has been modified to operate with the suppression of "hot" electrons that previously plagued these experiments.[15]

The room-temperature sample vapor entered the experimental chamber through a hypodermic needle and was ionized with vacuum ultraviolet (VUV) light from a hydrogen discharge lamp dispersed by a 1m normal incidence monochromator. The entrance and exit slits were set to 100 μm, which yield a resolution of 1 Å (8 meV at a photon energy of 10 eV). The VUV wavelengths were calibrated against the Lyman-α line. Ions and electrons are extracted in opposite directions with an electric field of 20V/cm.

The electrons are velocity focused[21,22] and detected by two Burle channeltrons, one of them located on the extraction axis and another located 5 mm to the side. Threshold electrons, with some contamination of energetic (hot) electrons, are detected by the first channeltron, whereas only hot electrons with a few millielectronvolts of kinetic energy perpendicular to the extraction axis are detected by the second channeltron. A hot electron free TPEPICO spectrum can be obtained by subtracting a fraction of the hot electron spectrum from the center spectrum, as described by Sztáray and Baer.[18]

The ions are mass analyzed by a modified linear TOF mass spectrometer in which they are accelerated to 100 eV in the first 5 cm long acceleration region and further accelerated to 260 eV in a short second region. The 30 cm long drift region is terminated by a 5 cm long region held at a lower voltage (ca. 180 V) to separate the fragment ions born in the drift region from long-lived parent ions. The ions are detected by a tandem Burle multichannel plate (MCP) detector.

The electron and ion signals are used as start and stop pulses, respectively, for measuring the ion time-of-flight (TOF), and the TOF for each coincidence event is stored on a multichannel pulse height analyzer. Separate TOF distributions are collected for the center and the off-center electron detectors. The "hot" electron free TPEPICO mass spectra (MS) were obtained by multiplying the off-center MS by a constant factor and subtracting these peaks from the center MS. As discussed in previous publications,[17−20] this factor is independent of the molecule, the photon energy, and remains constant as long as the collection efficiency of the two channeltron detectors remain the same. The peak areas of the "hot" electron corrected MS are plotted as breakdown diagrams, which are the fractional abundances of the ions formed by the dissociation of energy-selected parent ions as a function of the photon energy.

The product ion TOF distributions at energies close to the dissociation limit of the molecular ion contain information about the ion dissociation rates. If the dissociation is rapid, the peak shapes are symmetric and only their total areas are interesting. In this case we can obtain directly the corresponding breakdown diagram. On the other hand, if the dissociation reaction is slow, which is the case if the ion has a large number of vibrations and the activation energy is large, the daughter ion TOF peak shapes are asymmetric because the parent ions dissociate slowly in the first acceleration region. The analysis of this distribution reveals the dissociation rates as a function of the metastable ion internal energy.

B. Reagents. Tetramethylsilane (Me_4Si, purity >99.9%), hexamethyldisilane (Me_6Si_2, HMDS, purity >98%) and trimethylbromosilane (Me_3SiBr, purity >97%) were purchased from Sigma-Aldrich. Trimethyliodosilane was purchased from Fluka (Me_3SiI, purity ≥98%). These compounds were used without further purification. No impurities overlapping with interest signals were detected in the TOF spectra.

3. Theoretical Calculations and Simulation of Experimental Results

In the simulation of the experimental data, vibrational frequencies and rotational constants of the ground and transition states for relevant neutral and ionic species are required to calculate the thermal internal energy distribution of the molecule and the reaction rate constants. Thus, quantum chemical calculations were carried out using the Gaussian 03 package.[23] The ground-state geometries of the neutral and ionic species were optimized by using density functional theory (DFT), with the Becke 3 parameter and the Lee, Yang, Parr (B3LYP) functional,[24,25] and the 6-311G* basis set without symmetry restrictions. For the Me_3SiI molecule, the LANL2DZdp basis set was used with an effective core potential (ECP). The vibrational frequencies were obtained in these calculations without scaling. Approximate transition state (TS) vibrational frequencies were obtained by stretching the bond in question to approximately 4 Å at the B3LYP level of theory. The precise frequencies are not important because the calculated TS frequencies were used only as a starting point and were varied to fit the data.

The TOF distributions and breakdown diagrams were simulated using rate constants calculated with the statistical theory of unimolecular decay (RRKM), $k(E) = N^{\#}(E-E_0)/h\rho(E)$, where the numerator is the sum of internal energy states from the activation energy, E_0, to the total energy E, and $\rho(E)$ is the density of states at that energy.[26,27] Because our sample has a room temperature thermal energy distribution, the TOF distributions are characterized by a corresponding distribution of rate constants, which precludes us from extracting a single rate constants for each photon energy. We thus analyze the TOF distributions in terms of an assumed $k(E)$ curve and a thermal energy distribution. The $k(E)$ function was varied until a best fit was obtained. The simulations of the TOF distributions were carried out using the following information: the vibrational frequencies of the neutral sample that yield the sample's room-temperature internal energy distribution, the ion and transition state frequencies of the sample, the ionization energy, and the acceleration electric fields and drift distances of the ion time-of-flight system. The dissociation energies and the lowest three or four TS vibrational frequencies were varied to fit the simulation to the experimental data. Varying the TS frequencies and the onset energies in this quasi-microcanonical distribution is similar to varying the entropy of activation and activation energy in thermal systems. A single set of frequencies and energies were used to model all of the TOF distributions in Figure 4 and the breakdown diagram in Figure 6. The variable parameters were optimized using a downhill simplex method.[28,29] The calculated frequencies are provided as Supporting Information (see note at end of paper).

4. Results and Discussion

The dissociation onsets for the case of fast reactions are extracted by modeling the breakdown diagram (fractional

abundances of the various ions in the TPEPICO mass spectra). For slow reactions, the dissociation rate constants are extracted from the TPEPICO data by modeling the TOF distributions by a procedure to be described. By measuring the 0 K dissociation onset, E_0, for a dissociative photoionization process,

$$AB + h\nu \rightarrow AB^+ + e^- \rightarrow A^+ + B + e^- \qquad (1)$$

it is possible to derive the enthalpy of formation of one particular ion or molecule, using the well-established literature enthalpy of formation values for the others by

$$E_0 = \Delta_f H^\circ_{0K}(A^+) + \Delta_f H^\circ_{0K}(B) - \Delta_f H^\circ_{0K}(AB) \qquad (2)$$

Note that the eq 2 is valid only if all parameters are at 0 K. A similar equation holds at 298 K, but the 0 K onset, which can be determined unambiguously from the experimental results, must be converted to a 298 K value. The conversion of the enthalpy of formation from 0 to 298 K and vice versa can be made by means of the usual thermochemical cycle, given by

$$\Delta_f H^\circ_{0K} = \Delta_f H^\circ_{298K} - [H^\circ_{298K} - H^\circ_{0K}](\text{molecule/ion}) + [H^\circ_{298K} - H^\circ_{0K}](\text{elements}) \qquad (3)$$

where the value of $H^\circ_{298K} - H^\circ_{0K}$ for the molecule or ion was determined using DFT vibrational frequencies and "elements" refers to the sum of elements in their standard states, whose values were taken from the literature.[30,31] These same sources also provide the $\Delta_f H^\circ_{0K}$ of the atomic elements: 117.92 ± 0.06 kJ/mol for Br and 107.16 ± 0.04 kJ/mol for I.

The uncertainties for the dissociation onsets were obtained following the procedure described in previous studies,[19,32] which involves checking the flexibility of the fit upon variations in the adjustable parameters. The error limits in E_0 were then established by noting its value when the fit to the data became significantly worse.

A. Dissociation of Me_4Si, Me_3SiBr and Me_3SiI. Thermochemistry of the Trimethylsilyl Ion (Me_3Si^+). The dissociation process for the Me_4Si^+ and Me_3SiBr^+ ions are rapid ($k > 10^7$ s^{-1}), as evidenced by the symmetric shape of the TOF peaks in the mass spectra. These fast rates are also confirmed by calculated RRKM rate constants. The relative peak areas of the parent and daughter ions were plotted as a breakdown diagram, and the 0 K dissociation onsets (E_0) obtained from fitting these fractional ion abundances as function of the photon energy (Figures 1 and 2). The Me_4Si^+ ion dissociates to a single product, as shown in eq 4, at ion energies below 11 eV. The solid line is obtained by using the thermal energy distribution of the $SiMe_4$ molecule at 300 K and varying only a single parameter, which is the 0 K dissociation onset. The simulation assumes that ions below the dissociation limit are stable, and those above the dissociation limit dissociate instantaneously (or at least faster than the time scale of our experiment, which is some tens of nanoseconds). The 0 K onset for methyl loss from Me_4Si^+ is $E_0 = 10.243 \pm 0.010$ eV, which is 37 meV less than the onset reported by Szepes and Baer,[15] a difference that can probably be attributed to the previously mentioned "hot electron" contamination. Had we assumed the 1984 onset energy, the solid line in Figure 1 would have been shifted to higher energy by 37 meV, which is far beyond the experimental data. Using eq 2 with the auxiliary values listed in Table 1, we can obtain the enthalpy of formation at 0 K of the trimethylsilyl ion, $\Delta_f H^\circ_{0K}(Me_3Si^+) = 636.1 \pm 3.4$ kJ/mol.

$$Me_4Si + h\nu \rightarrow Me_4Si^+ + e^- \xrightarrow{\text{fast}} Me_3Si^+ + Me^\bullet + e^- \qquad (4)$$

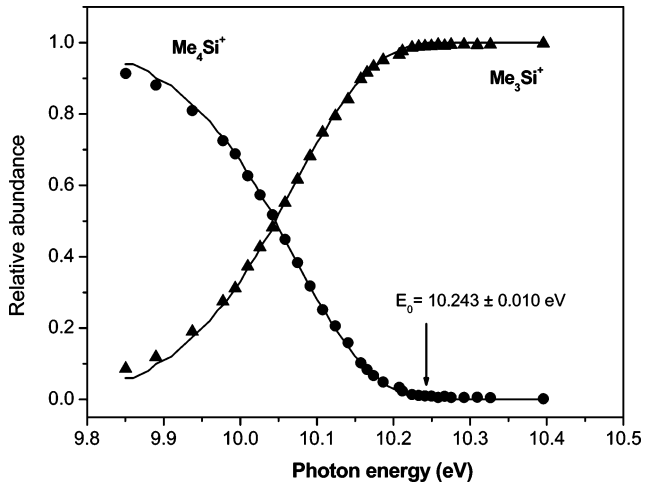

Figure 1. Breakdown diagram for $SiMe_4^+$. The solid line through the experimental points is obtained by modeling a fast dissociation with a room temperature (300 K) thermal energy distribution. The indicated onset is derived from the fit.

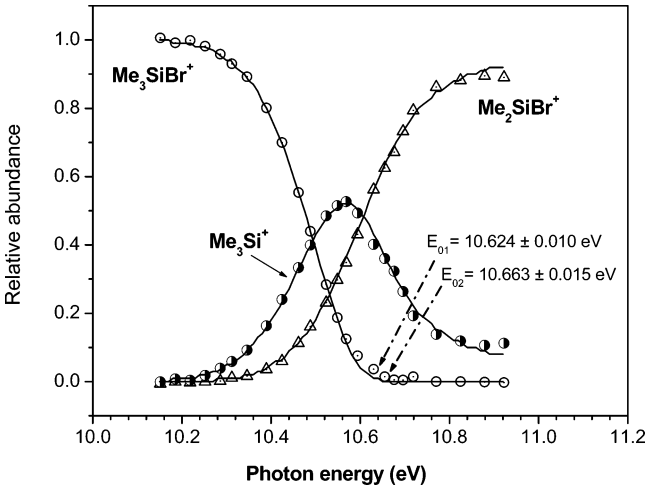

Figure 2. Breakdown diagram for $SiMe_3Br^+$. The solid lines through the experimental points are obtained by modeling a fast dissociations with a room temperature thermal energy distribution. The higher energy methyl loss onset required the fitting of transition state frequencies. The indicated onsets are derived from the fit.

Reaction 5 shows the parallel dissociation steps for Me_3SiBr^+. The first dissociation onset at 0 K is $E_{01} = 10.624 \pm 0.010$ eV and corresponds to the Br loss. The simulated fit is obtained,

$$Me_3SiBr + h\nu \rightarrow Me_3SiBr^+ + e^- \rightarrow \begin{cases} Me_3Si^+ + Br^\bullet + e^- & E_{01} \\ Me_2SiBr^+ + Me^\bullet + e^- & E_{02} \end{cases} \qquad (5)$$

as for the Me_4Si case, by varying only a single parameter, which is the 0 K dissociation onset. The second dissociation channel at $E_{02} = 10.663 \pm 0.015$ eV, corresponds to the methyl loss reaction, which is observed in competition with the first fragmentation channel. To fit the breakdown diagram (Figure 2), the transition state (TS) frequencies of the two reaction channels are required. Because the reaction is fast, we do not know the absolute rate constant. Thus we fix the TS frequencies for the first channel while varying the five lowest frequencies for the methyl loss reaction along with the 0K onset, E_{02}, until the fit in Figure 2 is obtained. The determination of the second onset thus involves varying two parameters. The measurements of Szepes and Baer[15] reported 10.70 and 10.79 eV for these

TABLE 1: Auxiliary and Derived Thermochemical Data (in kJ/mol)

	$\Delta_f H^\circ_{0K}$	$(H^\circ_{298K} - H^\circ_{0K})^a$	$\Delta_f H^\circ_{298K}{}^b$	$\Delta_f H^\circ_{298K}$ (lit. value)
Me_4Si	-201.9^c	26.92		-233.2 ± 3.2^d
Me_3SiBr	-266.4^c	25.64		-297.5 ± 4.1^e
Me_3SiI	-196.9^c	25.96		-222 ± 4^f
Me_6Si_2	-257.9^c	43.11		-303.7 ± 5.5^g
Me_3Si^+	638.6 ± 2.3^b	23.16	617.3 ± 2.3	610 ± 20,^{h}624 ± 6^i
Me_2SiBr^+	604.7 ± 4.4^b	21.15	590.3 ± 4.4	
$Me_5Si_2^+$	524.0 ± 6.2^b	38.78	487.6 ± 6.2	
$Me_3Si^\bullet$	36.5 ± 6.6^b	21.95	14.0 ± 6.6	14 ± 7^j
			14.8 ± 2.0^m	16.4 ± 6^k
				13^l
$Me^\bullet$	150.3 ± 0.4^n			

[a] Calculated using DFT method described in text. [b] Determined from current TPEPICO dissociation onsets. [c] Converted from the 298 K literature value. [d] Steele.[10] [e] Cox and Pilcher.[33] [f] Revised and modified by Becerra & Walsh[4] from results obtained by Doncaster and Walsh.[34] [g] Pilcher et al.[9] [h] Suggested by Walsh.[35] [i] Old TPEPICO data by Szepes and Baer using updated ancillary heats of formation. [j] Bullock et al.[6] [k] Kalinovski et al.[4] [l] Calculated by Allendorf and Melius.[36] [m] Average value of the three best experimental determinations. [n] From Weitzel et al.[37] and Blush et al.[38]

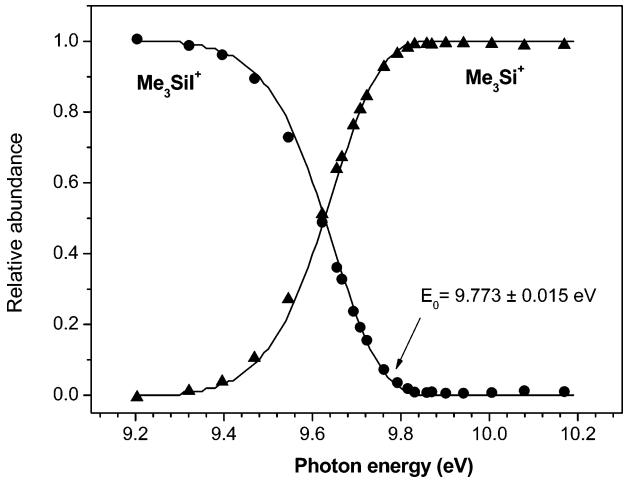

Figure 3. Breakdown diagram for $SiMe_3I^+$. The solid line through the experimental points is obtained by modeling the TOF distributions (not shown) as well as the breakdown diagram. The slightly slow rate at threshold was taken into account in determining the indicated onset energy.

two onsets, which are significantly higher than the present measurements. The reason for this is certainly the effect of the "hot" electrons, which significantly contaminated the old data for this molecule because the dissociation onsets are in a Franck−Condon gap where the yield of threshold electrons is very small. This is made evident in the parent ion signal, which disappears in Figure 2 at a photon energy of 10.62 eV. In the old data, the parent ion signal at that energy was 35% and the signal did not go down to baseline even at 11 eV.

These onset values permit us to obtain the 0 K enthalpy of formation for Me_3SiBr^+ and Me_3Si^+ ions: $\Delta_f H^\circ_{0K}(Me_2SiBr^+) = 604.7 \pm 4.4$ kJ/mol and $\Delta_f H^\circ_{0K}(Me_3Si^+) = 640.7 \pm 4.2$ kJ/mol, respectively.

The dissociation process for Me_3SiI (reaction 6) in the range 9.20−10.20 eV involves a single product ion,

$$Me_3SiI + h\nu \rightarrow Me_3Si^+ + I^\bullet + e^- \qquad (6)$$

This reaction is sufficiently slow to result in slightly asymmetric TOF peaks for the daughter ions at low ion internal energies. The 0 K dissociation onset (E_0) is obtained from fitting both the breakdown diagram (Figure 3) and the TOF distributions (not shown here). The resulting onset for I loss is $E_0 = 9.773 \pm 0.015$ eV. The slow rate constant has shifted the onset to lower energies relative to the fast reactions in Figures 1 and 2. This onset value permits us to calculate the 0 K enthalpy of formation for Me_3Si^+ ion, $\Delta_f H^\circ_{0K}(Me_3Si^+) = 638.9 \pm 4.3$ kJ/mol.

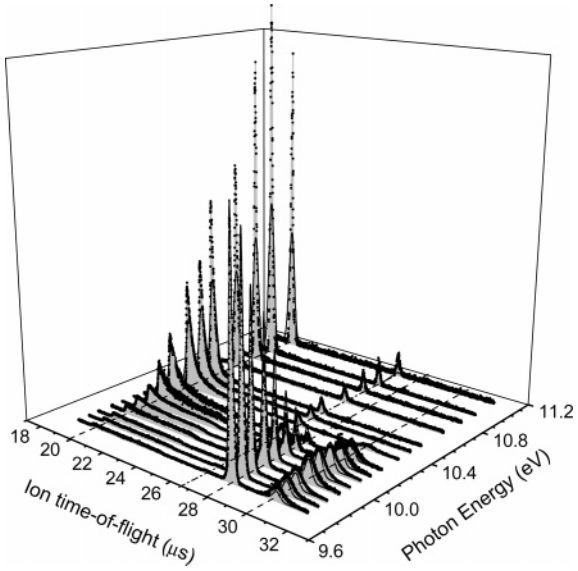

Figure 4. Time-of-flight distributions for the hexamethyldisilane ions at several energies showing the change as the dissociation rates increase with increasing ion energy. The solid lines through the experimental points were based on modeling of the data in which the thermal energy distribution and the rate constants (Figure 7) were used.

It is gratifying to note that the enthalpies of formation for the trimethylsilyl ion obtained from the Me_4Si, Me_3SiBr and Me_3SiI breakdown diagrams are very close. This excellent agreement means that the thermochemistry of these three compounds is self-consistent. We suggest the average value of $\Delta_f H^\circ_{0K}(Me_3Si^+) = 638.6 \pm 2.3$ kJ/mol as an accurate enthalpy of formation at 0 K, which converts to $\Delta_f H^\circ_{298K}(Me_3Si^+) = 617.3 \pm 2.3$ kJ/mol at 298 K. This value is in agreement with the value suggested by Walsh,[35] which was estimated, with a very high uncertainty, as 610 ± 20 kJ/mol from a compilation of several experimental results.

B. Dissociation of Me_6Si_2 (HMDS). Thermochemistry of the Trimethylsilyl Radical ($Me_3Si^\bullet$). The dissociation of Me_6Si_2 (reaction 7) takes place via two parallel channels,

$$Me_6Si_2 + h\nu \rightarrow \begin{cases} Me_5Si_2^+ + Me^\bullet + e^- & E_{01} \\ Me_3Si^+ + Me_3Si^\bullet + e^- & E_{02} \end{cases} \qquad (7)$$

The TOF mass spectra of HMDS were acquired in the photon energy range of 9.60−11.10 eV and their TOF distributions at various energies are shown in Figure 4. Figure 5 shows one of these time-of-flight distributions, where one can see the peak at 27.9 μs corresponding to the parent ion ($Me_6Si_2^+$, m/z 146), two asymmetric peaks corresponding to daughter ions formed by cleavage of the Si−Si or Si−C bonds: Me_3Si^+ (m/z 73, 19.8 μs) and $Me_5Si_2^+$ (m/z 131, 26.5 μs), respectively. The asymmetric Me_3Si^+ peak is a result of ions that dissociate in the 5 cm long acceleration region. Each position of dissociation maps onto a final ion TOF. The asymmetric peak exhibits a step at 24 μs, which corresponds to ions that dissociate at the exit of the first acceleration region. The solid line through the data points models this step perfectly.

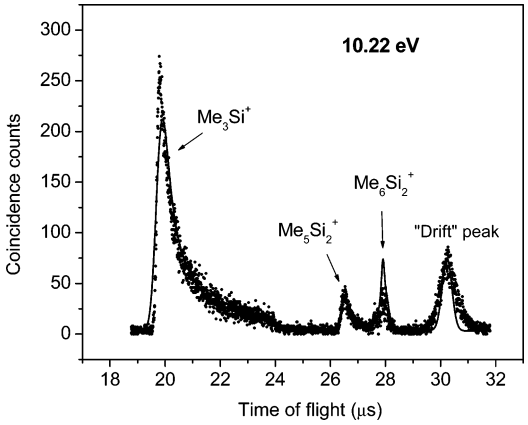

Figure 5. Time-of-flight distribution of the hexamethyldisilane ions at 10.22 eV, showing the fit of the model to the asymmetric peak shapes. The "drift" peak is a result of ions that dissociate in the drift region.

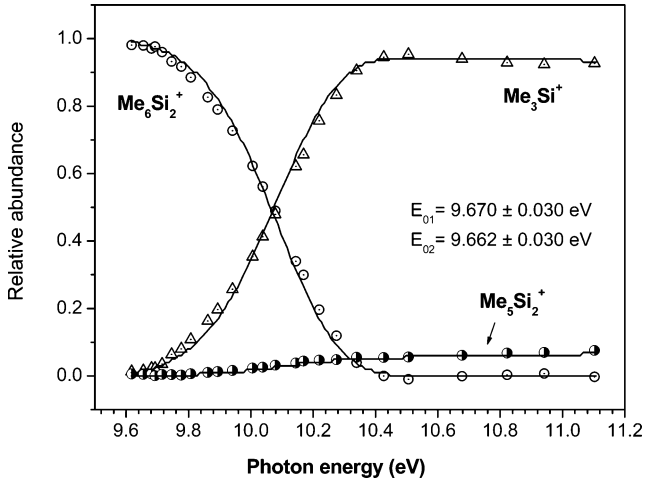

Figure 6. Breakdown diagram for hexamethyldisilane. The solid lines through the experimental points were derived by fitting both the TOF distributions in Figure 4 as well as the breakdown diagram.

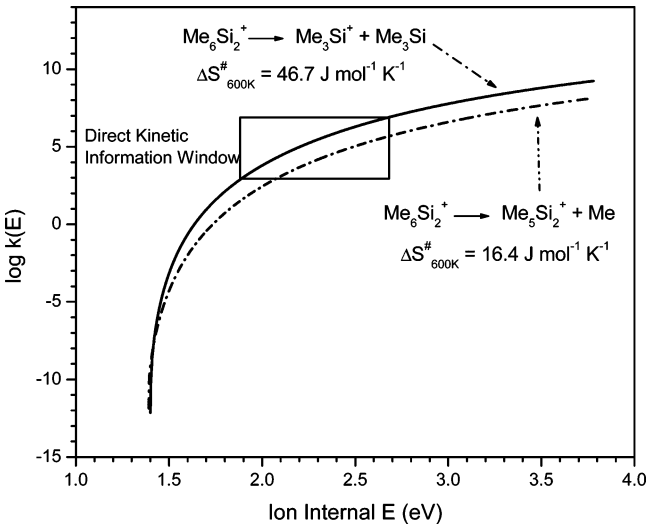

Figure 7. RRKM rate constants that fit both the TOF distributions and the breakdown diagram for hexamethyldisilane.

The somewhat broader peak ("drift peak") at 30.2 μs is associated with fragment ions (mostly Me_3Si^+ ions) that were formed in the 30 cm long drift region. This "drift" peak appears after the parent ions in the TOF spectrum because the final 5 cm drift region is at a voltage lower than that of the main drift tube. In the absence of this extra drift region, the fragment ions that are produced in the drift region, which have the same velocity (although different kinetic energies), would have the same TOF as the parent ion. However, the deceleration field slows the fragment ions down more than the parent ions because they have less kinetic energy than the parent ions, thereby yielding a TOF that is longer than that of the parent ions. This peak is also broader for several reasons that are not included in the modeling of this peak. Perhaps chief among them is the kinetic energy release during the dissociation step that yields a distribution of ion kinetic energies. The shape of this peak is less important than its total area.

The fragment ion TOF distribution can be understood in terms of an exponential decay of the parent ion in which the exponential is directly measured in the asymmetric TOF peak up to a time that corresponds to the parent ion acceleration time in the first acceleration region (t_1), and the "drift peak", which represents the integrated signal from t_1 to t_2, where t_2 is the total parent ion flight time up to the deceleration region. All ions that live longer than t_2 would appear as parent ions.

The fractional abundances of the parent and fragment ions are shown in the breakdown diagram in Figure 6. In this breakdown diagram, the "drift" peak is added onto the parent ion so that only those ions that dissociated in the first 5 cm (8.7 μs) acceleration region are counted as product ions.

The TOF distributions in Figures 4 and 5 and the breakdown diagram in Figure 6 are modeled by varying the dissociation onsets of the Si−Si and the Si−Me bond break reactions as well as the transition state vibrational frequencies, which determine the rate constants, $k(E)$ for these two reactions. The solid lines in these three figures are the result of this modeling. The rate constants shown in Figure 7 were the optimum $k(E)$ functions that fitted all of the data in Figures 4−6. The metastable energy range over which we can determine the dissociation rate constants extends from 9.8 to 10.4 eV, an energy range that is shown as a box in Figure 7.

The derived 0 K dissociation onsets for this HMDS are $E_{01} = 9.662 \pm 0.030$ eV (methyl loss) and $E_{02} = 9.670 \pm 0.030$ eV (Si−Si bond cleavage). Note that these onsets are located at the beginning of the breakdown diagram in Figure 6. This is a reflection of the large kinetic shift for this reaction. The previous TPEPICO study of Szepes and Baer[15] reported onsets that are 92 meV lower (Me loss) and 100 meV higher (Si−Si cleavage) than the present values but are within their quoted errors of 0.10 eV. The large error bars in the older TPEPICO results can be ascribed to several factors. The old data were collected with a single acceleration region TOF in which it was difficult to resolve the methyl loss peak. Second, the hot electron contamination affected the derived rate constants especially at the high energy end so that the rate constants could only be measured between 10^4 and 10^6 s^{-1}. In addition, the much more sophisticated modeling of the current data in terms of the thermal energy distribution, rather than simply the average thermal energy is particularly important here because the distribution is rather broad in the case of HMDS as a result of the many vibrational degrees of freedom.

The activation entropies of the two dissociation channels, calculated at 600 K using the transition state frequencies obtained from fitting the data, were 16.4 and 46.7 J·mol^{-1}·K^{-1} for the Si−Me and Si−Si bond breaking steps, respectively. Both are positive, which indicates that these reactions proceed via loose transition states, especially the second channel (Si−Si bond breaking step). The $k(E)$ curves in Figure 7 reflect this difference in the activation entropies in that the Si−Si bond

breaking reaction rate increases more rapidly than the Si−Me bond breaking rate.

The measured 0 K dissociation limits of HMDS (E_{01} and E_{02}) can now be used along with the enthalpies of formation of HMDS (Table 1) and Me_3Si^+ (obtained in this work) to calculate $\Delta_f H^\circ_{0K}$ of the $Me_5Si_2^+$ ion and trimethylsilyl radical, $Me_3Si^\bullet$. These are $\Delta_f H^\circ_{0K}(Me_5Si_2^+) = 524.0 \pm 6.2$ kJ/mol and $\Delta_f H^\circ_{0K}(Me_3Si^\bullet) = 36.5 \pm 6.6$ kJ/mol. The latter value converts to $\Delta_f H^\circ_{298K}(Me_3Si^\bullet) = 14.0 \pm 6.6$ kJ/mol. This value is identical to one reported by Bullock, Walsh and King,[6] in which the kinetics of HMDS pyrolysis was reinvestigated using the technique of very-low-pressure pyrolysis, thereby correcting substantially, the earlier studies by Walsh.[11,39] This value is also very close to one calculated by Allendorf and Mellius[36] from a theoretical ab initio study (BAC-MP4 (STDQ) method). Finally, our value is in agreement with the 16.4 ± 6.0 kJ/mol, reported by Marshall and co-workers,[7,8,40] in which the forward and reverse rate measurements of the $Me_3Si + HBr$ $Me_3SiH + Br^\bullet$ reaction were measured over a broad temperature range. The trimethylsilyl radical heat of formation was thus determined from the directly measured heat of reaction.

We have then three related measurements of the $Me_3Si^\bullet$ heat of formation. These are based on the following measured reaction enthalpies:

$$Me_3SiSiMe_3 \rightarrow 2Me_3Si^\bullet \quad \text{pyrolysis}$$

$$Me_3SiSiMe_3 \rightarrow Me_3Si^\bullet + Me_3Si^+ \quad \text{TPEPICO}$$

$$Me_4Si \rightarrow Me_3Si^\bullet + Me^\bullet \quad \text{TPEPICO}$$

$$Me_3SiH + Br^\bullet \rightleftarrows Me_3Si^\bullet + HBr \quad \text{kinetics}$$

Extraction of the trimethylsilyl heat of formation depends on the heats of formation of $Me_3SiSiMe_3$, Me_4Si, and Me_3SiH, as well as $Br^\bullet$, $CH_3^\bullet$, and HBr. The Me_3Si^+ ion is an intermediate in the TPEPICO determination. In fact, our TPEPICO results can be rewritten in the form of the following reaction: $Me_3SiSiMe_3 + Me^\bullet \rightarrow Me_3Si^\bullet + Me_4Si$, which shows that our derived $Me_3Si^\bullet$ heat of formation is based on both the HMDS and the Me_4Si. The fact that the three measurements agree to within their experimental uncertainties indicates that methylsilane heats of formation are now well established. In addition, it means that the respective experimental techniques have been perfected and yield reliable results. Although the error limits on each of the trimethylsilyl radicals are 7 kJ/mol, the three measurements (14.0, 14.0, and 16.4) agree to much better than this. It seems that the average enthalpy of formation for trimethylsilyl radical is much more accurate than each individual one, and we thus claim that the heat of formation, $\Delta_f H^\circ_{298K}(Me_3Si^\bullet) = 14.8 \pm 2.0$ kJ/mol.

It is perhaps surprising that our analysis of the HMDS rate data yields a trimethylsilyl radical heat of formation that agrees so well with other determinations. Our value is based on an E_0 whose value was determined from the extrapolation of the RRKM theory rate constants to the dissociation onset shown in Figure 7. For the extrapolation of about 0.45 eV to yield an onset energy accurate to 0.030 eV is quite remarkable. Troe et al. [41] have recently suggested that such extrapolations are subject to large errors, especially in the case of H loss from the benzene ion, which proceeds by a somewhat tight transition state. The reason for this, in the framework of the variational RRKM theory,[42,43] is the transition state is not stationary but moves to larger bond distances as the energy is lowered. In contrast to H loss reactions, the large polarizability of the trimethylsilyl radical may shift the transition state to a larger Si−Si bond distance so that even at an energy of 0.45 eV above the dissociation limit, the transition state is already very loose so that its energy corresponds to that of the dissociated products. It should also be noted that our rate constant measurements span a range of almost 4 orders of magnitude, from 10^3 to 5×10^6 s^{-1}, which greatly improves our ability to extrapolate the $k(E)$ function.

TABLE 2: Bond Dissociation Enthalpies (in kJ/mol)

	ΔH_{298K}	ΔH_{298K} (lit. values)
Me_3Si-H	396.2 ± 4.2^a	396,[f] 398 ± 6,[g] 397.4 ± 2^h
Me_3Si-Me	395.1 ± 3.5^b	392.5,[f] 394 ± 8^i
Me_3Si-Cl	490.1 ± 3.2^c	490 ± 8^i
Me_3Si-Br	424.2 ± 4.3^c	425 ± 8^i
Me_3Si-I	343.6 ± 4.2^d	344 ± 8^i
$Me_3Si-SiMe_3$	333.3 ± 5.8^e	332 ± 12^j

[a] Calculated using the $\Delta_f H^\circ_{298K}(Me_3SiH) = -163 \pm 4$ kJ/mol from Doncaster and Walsh.[48] [b] Taking $\Delta_f H^\circ_{298K}(Me_4Si)$ from Steele.[10] [c] Taking $\Delta_f H^\circ_{298K}(Me_3SiCl)$ from Cox and Pilcher.[33] [d] Taking $\Delta_f H^\circ_{298K}(Me_3SiI)$ from Becerra and Walsh.[4] [e] Taking $\Delta_f H^\circ_{298K}(Me_6Si_2)$ from Pilcher et al.[9] [f] Allendorf and Melius.[36] [g] Ding and Marshall.[7] [h] Kalinovski et al.[8] [i] Becerra and Walsh.[4] [j] Bullock et al.[6]

C. Measurement of Bond Dissociation Enthalpies (ΔH_{298K}). The enthalpy of reaction 8 (homolytic bond cleavage at 298 K), permits us to calculate the bond dissociation enthalpy, ΔH_{298K}, for Me_3Si-X species,

$$Me_3SiX \rightarrow Me_3Si^\bullet + X^\bullet \qquad \Delta_r H = \Delta H_{298K} \qquad (8)$$

Table 2 shows the ΔH_{298K} values for Me_3Si-X (X = H, Me, Cl, Br, I and $SiMe_3$) calculated, by eq 8, using the enthalpy of formation of each molecule derived in this work (i.e., trimethylsilyl radical) as well as from the literature (ref 31, Table 1). From these results we deduce the following observations,

(a) ΔH_{298K} values for the halogen trimethylsilanes reflect the expected trends of decreasing bond enthalpy down the periodic column: Si−Cl > Si−Br > Si−I.

(b) ΔH_{298K} for Me_3Si-H is essentially the same as that for Me_3Si-Me, which is quite different from the C−H and C−C bond energy trends. This observation was already reported by Walsh,[11] Kanabus-Kaminska,[44] and Brauman and co-workers,[45] on the basis of a variety of experimental studies. Although they generalized this lack of substituent effect in organosilanes, the trend is not uniform. For instance, methyl substitution slightly increases the Si−H bond energy, as can be seen in Figure 8 (values taken from Table 2 and the literature) where the H_3Si-H and Me_3Si-H bond enthalpies increase from 384.1 ± 2.0 to 396.2 ± 4.2 kJ/mol,[47] an increase of 12.1 kJ/mol. But in general, the lack of methyl substitution effect in Me_3Si-H, according to Wetzel et al.,[45] is a consequence of the stability of trimethylsilyl radical, which is essentially unaffected by alkyl substitution.

(c) Comparison of the Si−Si bond dissociation enthalpy of $H_3Si-SiH_3$ (321 ± 5 kJ/mol)[7] with the measured bond energy in $Me_3Si-SiMe_3$ (333.3 ± 5.8 kJ/mol) confirms also that methyl substitutions slightly increases the Si−Si bond enthalpies. This increment (12.3 kJ/mol) is practically the same as that for the Si−H bond enthalpies.

The small alkyl substituent effects in organosilanes and the opposite effects in carbon compounds (known as "methyl group inductive effect") are shown in Figure 8. These differences can be rationalized[8,11] by taking into account the difference in the Pauling electronegativities of silicon and carbon and their relation to the stability of their corresponding radicals. On the other hand, the high value of $\Delta H_{298K}(Me_3Si-Me)$ in comparison

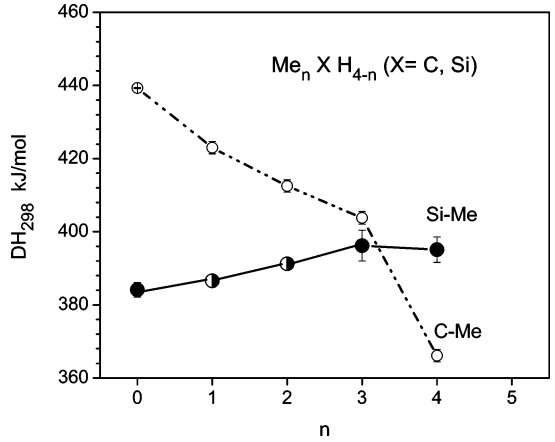

Figure 8. Bond dissociation enthalpies (X−H for $n \leq 3$), ΔH_{298K}, for (a) hydrocarbons (dots), values taken from Blanksby and Ellison,[46] and (b) methylsilanes (solid line), values taken from Seetula et al.[47] ($n = 0$) and Allendorf and Melius[36] ($n = 1, 2$).

to $\Delta H_{298K}(Me_3C-Me)$ (a difference of 29 kJ/mol) can be explained, according to theoretical study of Hirao et al.[49] in terms of shielding of the valence electrons by the core electrons. The shielding for the C atoms involves only spherically symmetric "s" electrons, whereas for Si, the shielding of the valence p electrons is exerted by the p-like electrons in the core. Therefore, the ΔH_{298K} for the C−Me bond will be lower than that for Si−Me. Another contribution to the increased Si−Me bond enthalpy, could be the presence of the virtual "d" electrons, which yield an important contribution to the electron correlation of Si derivatives.[49]

5. Conclusions

The derived thermochemistry from dissociative photoionization experiments have been studied for a set of silane compounds: Me_4Si, Me_6Si_2, and Me_3SiX, (X = Br, I), by using the threshold photoelectron and photoion coincidence (TPEPICO) technique. From the analysis of breakdown diagrams and the simulation of time-of-flight spectra (particularly for the metastable $Me_6Si_2^+$ ions) we have obtained accurate dissociation onsets, which were used to find a $\Delta_f H^\circ_{298}(Me_3Si^+)$ of 617.3 ± 2.3 kJ/mol. This value is then used to determine the trimethylsilyl radical heat of formation of 14.0 ± 6.6 kJ/mol. By combining this with other values that agree very well, we propose an average enthalpy of formation of $\Delta_f H^\circ_{298K}(Me_3Si^\bullet) = 14.8 \pm 2.0$ kJ/mol with considerably lower error limits. Using the new value of $\Delta_f H^\circ_{298K}(Me_3Si^\bullet)$, we have calculated several bond dissociation enthalpies (ΔH_{298K}) and can confirm the small methyl substituent effects on Si−H bond dissociation energy. These same effects have been corroborated on Si−Si bond dissociation.

Acknowledgment. We thank the U.S. Department of Energy for support this work. J.Z.D. acknowledges the Ministerio de Educación, Cultura y Deporte of Spain, for the PR2004-0031 Grant. We also thank Prof. Bálint Sztáray of the Eötvös Loránd, University Budapest, for help in the modeling of the experimental data.

Supporting Information Available: Calculated (B3LYP/6-311 G**) harmonic vibrational frequencies required for the data analysis are available free of charge via the Internet at http://pubs.acs.org.

References and Notes

(1) Jasinski, J. M.; Gates, S. M. *Acc. Chem. Res.* **1991**, *24*, 9.
(2) Jasinski, J. M.; Meyerson, B. S.; Scott, B. A. *Annu. Rev. Phys. Chem.* **1987**, *38*, 109.
(3) Jasinski, J. M.; Becerra, R.; Walsh, R. *Chem. Rev.* **1995**, *95*, 1203.
(4) Becerra R.; Walsh, R. *The Chemistry of Organic Silicon Compounds*; John Wiley & Sons: New York, 1998; Chapter 4.
(5) Krasnoperov, L. N.; Niiranen, J. T.; Gutman, D.; Melius, C. F.; Allendorf, M. D. *J. Phys. Chem.* **1995**, *99*, 14347 and references therein.
(6) Bullock, W. J.; Walsh, R.; King, K. D. *J. Phys. Chem.* **1994**, *98*, 2595.
(7) Ding, L.; Marshall, P. *J. Am. Chem. Soc.* **1992**, *114*, 5754.
(8) Kalinovski, I. J.; Gutman, D.; Krasnoperov, L. N.; Goumri, A.; Yuan, W. J.; Marshall, P. *J. Phys. Chem.* **1994**, *98*, 9551.
(9) Pilcher, G.; Luisa, M.; Leitao, P.; Yang, M.; Walsh, R. *J. Chem. Soc. Faraday Trans.* **1991**, *87*, 841.
(10) Steele, W. V. *J. Chem. Therm.* **1983**, *15*, 595.
(11) Walsh, R. *Acc. Chem. Res.* **1981**, *14*, 246.
(12) Pedley, J. B.; Rylance, J. *Sussex-NPL Computer Analysed Thermochemical Data: Organic and Organometallic Compounds*; University of Sussex: Sussex, U.K., 1977.
(13) Murphy, M. K.; Beauchamp, J. L. *J. Am. Chem. Soc.* **1977**, *99*, 2085.
(14) Ruscic, B.; Pinzon, R. E.; Morton, M. L.; Laszevski, G.; Bittner, S. J.; Nijsure, S. G.; Amin, K. A.; Minkoff, M.; Wagner, A. F. *J. Phys. Chem. A* **2004**, *108*, 9979.
(15) Szepes, L.; Baer, T. *J. Am. Chem. Soc.* **1984**, *106*, 273.
(16) Baer, T.; Li, Y. *Int. J. Mass Spectrom.* **2002**, *219*, 381.
(17) Baer, T.; Sztáray, B.; Kercher, J. P.; Lago, A. F.; Bodi, A.; Scull, C.; Palathinkal, D. *Phys. Chem. Chem. Phys.* **2005**, *7*, 1507.
(18) Sztáray, B.; Baer, T. *Rev. Sci. Instrum.* **2003**, *74*, 3763.
(19) Bodi, A.; Kercher, J. P.; Baer, T.; Sztáray, B. *J. Phys. Chem. B* **2005**, *109*, 8393.
(20) Fogleman, E. A.; Koizumi, H.; Kercher, J. P.; Sztáray, B.; Baer, T. *J. Phys. Chem. A* **2004**, *108*, 5288.
(21) Chandler, D. W.; Parker, D. H. *Adv. Photochem.* **1999**, *25*, 59.
(22) Suits, A. G., Continetti, R. E., Eds. *Imaging in Chemical Dynamics*; American Chemical Society: Washington, DC, 2001.
(23) Frisch, M. J.; Trucks, G. W.; Schlegel, H. B.; Scuseria, G. E.; Robb, M. A.; Cheeseman, J. R.; Montgomery, J. A., Jr.; Vreven, T.; Kudin, K. N.; Burant, J. C.; Millam, J. M.; Iyengar, S. S.; Tomasi, J.; Barone, V.; Mennucci, B.; Cossi, M.; Scalmani, G.; Rega, N.; Petersson, G. A.; Nakatsuji, H.; Hada, M.; Ehara, M.; Toyota, K.; Fukuda, R.; Hasegawa, J.; Ishida, M.; Nakajima, T.; Honda, Y.; Kitao, O.; Nakai, H.; Klene, M.; Li, X.; Knox, J. E.; Hratchian, H. P.; Cross, J. B.; Bakken, V.; Adamo, C.; Jaramillo, J.; Gomperts, R.; Stratmann, R. E.; Yazyev, O.; Austin, A. J.; Cammi, R.; Pomelli, C.; Ochterski, J. W.; Ayala, P. Y.; Morokuma, K.; Voth, G. A.; Salvador, P.; Dannenberg, J. J.; Zakrzewski, V. G.; Dapprich, S.; Daniels, A. D.; Strain, M. C.; Farkas, O.; Malick, D. K.; Rabuck, A. D.; Raghavachari, K.; Foresman, J. B.; Ortiz, J. V.; Cui, Q.; Baboul, A. G.; Clifford, S.; Cioslowski, J.; Stefanov, B. B.; Liu, G.; Liashenko, A.; Piskorz, P.; Komaromi, I.; Martin, R. L.; Fox, D. J.; Keith, T.; Al-Laham, M. A.; Peng, C. Y.; Nanayakkara, A.; Challacombe, M.; Gill, P. M. W.; Johnson, B.; Chen, W.; Wong, M. W.; Gonzalez, C.; Pople, J. A. *Gaussian 03*, revision A.1.; Gaussian, Inc.: Pittsburgh, PA, 2004.
(24) Becke, A. D. *J. Chem. Phys.* **1993**, *98*, 5648.
(25) Lee, C.; Yang, W.; Parr, R. G. *Phys. Rev.* **1988**, *B37*, 785.
(26) Baer, T.; Hase, W. L. *Unimolecular Reaction Dynamics: Theory and Experiments*; Oxford University Press: New York, 1996.
(27) Marcus, R. A.; Rice, O. K. *J. Phys. Colloid Chem.* **1951**, *55*, 894.
(28) Nelder, J. A.; Mead, R. *Comput. J.* **1965**, *7*, 303.
(29) Press, W. H.; Teukolsky, S. A.; Vetterling, W. T.; Flannery, B. P. *Numerical recipes in C. The art of scientific computing*, 2nd ed.; Cambridge University Press: Cambridge, U.K., 1992; p 408.
(30) Wagman, D. D.; Evans, W. H. E.; Parker, V. B.; Schum, R. H.; Halow, I.; Mailey, S. M.; Churney, K. L.; Nuttall, R. L. *The NBS Tables of Chemical Thermodynamic Properties*, *J. Phys. Chem. Ref. Data Vol. 11 Suppl. 2*, NSRDS: U.S. Government Printing Office: Washington, DC, 1982.
(31) Chase, M. W., Jr. *NIST-JANAF Thermochemical Tables*, 4th ed.; 1998; pp 1−1951.
(32) Li, Y.; Sztáray, B.; Baer, T. *J. Am. Chem. Soc.* **2001**, *123*, 9388.
(33) Cox, J. D.; Pilcher, G. *Thermochemistry of organic and organometallic compounds*; Academic Press: London, 1970.
(34) Doncaster, A. M.; Walsh, R. *J. Phys. Chem.* **1979**, *83*, 3037.
(35) Walsh, R. *J. Phys. Chem.* **1986**, *90*, 389.
(36) Allendorf, M. D.; Melius, C. F. *J. Phys. Chem.* **1992**, *96*, 428.
(37) Weitzel, K. M.; Malow, M.; Jarvis, G. K.; Baer, T.; Song, Y.; Ng, C. Y. *J. Chem. Phys.* **1999**, *111*, 8267.
(38) Blush, J. A.; Chen, P.; Wiedmann, R. T.; White, M. G. *J. Chem. Phys.* **1993**, *98*, 3557.
(39) Walsh, R. *Energetics of Organometallic Species*; Kluver: Dordrecht, The Netherlands, 1992; Chapter 11, p 171.

(40) Goumri, A.; Yuan, W. J.; Marshall, P. *J. Am. Chem. Soc.* **1993**, *115*, 2539.
(41) Troe, J.; Ushakov, V. G.; Viggiano, A. A. *J. Phys. Chem. A* **2006**, *110*, 1491.
(42) Truhlar, D. G.; Garrett, B. C. *Annu. Rev. Phys. Chem.* **1984**, *35*, 159.
(43) Lifshitz, C. *Adv. Mass Spectrom.* **1989**, *11*, 713.
(44) Kanabus-Kaminska, J. M.; Hawari, J. A.; Griller, D.; Chatgilialoglu, C. *J. Am. Chem. Soc.* **1987**, *109*, 5267.
(45) Wetzel, D. M.; Salomon, K. E.; Berger, S.; Brauman, J. I. *J. Am. Chem. Soc.* **1989**, *111*, 3835.
(46) Blanksby, S. J.; Ellison, G. B. *Acc. Chem. Res.* **2003**, *36*, 255.
(47) Seetula, J. A.; Feng, Y.; Gutman, D.; Seakins, P. W.; Pilling, M. J. *J. Phys. Chem.* **1991**, *95*, 1658.
(48) Doncaster, A. M.; Walsh, R. *J. Chem. Soc. Faraday Trans. 2* **1986**, *82*, 707.
(49) Lie, W.; Fedorov, D. G.; Hirao, K. *J. Phys. Chem. A* **2002**, *106*, 7057.